Polym. Bull. (2009) 62:615–627
DOI 10.1007/s00289-009-0046-y

ORIGINAL PAPER

Preparation of silica microtubes by surface-initiated atom transfer radical polymerization from microfiber templates

Zhongfu Huang · Yiwang Chen · Weihua Zhou · Zupeng Guo

Received: 19 December 2007 / Revised: 4 July 2008 / Accepted: 21 January 2009 /
Published online: 6 February 2009
© Springer-Verlag 2009

Abstract Poly(methyl methacrylate-*co*-vinylbenzyl chloride), P(MMA-*co*-VBC) microfibers (with submicron diameters) of about 1 μm in size were prepared by electrospinning. Silyl-functional groups were introduced onto the P(MMA-*co*-VBC) microfibers templates via surface-initiated atom transfer radical polymerization of 3-(trimethoxysilyl)propyl methacrylate. The silyl groups were then converted into a silica shell, approximately 0.25 μm thick, via a reaction with tetraethoxysilane in ethanolic ammonia. Hollow silica microfibers were finally generated by thermal decomposition of the P(MMA-*co*-VBC) template cores. Scanning electron microscopy and transmission electron microscopy were used to characterize the intermediate products and the hollow microtubes. Fourier-transform infrared spectroscopy results indicated that the polymer cores were completely decomposed. The microfibers were characterized by X-ray photoelectron spectroscopy, X-ray diffraction and the thermal gravimetric analysis.

Keywords Microfibers · Atom transfer radical polymerization · Silica microtubes · Templates

Introduction

In the last decade, extensive research has been undertaken in the synthesis of hollow macro- or nanotubes. Hollow nanotubes currently attract considerable interest because of their excellent properties such as low density, large specific surface area and good stability as well as their surfaces accessible and modified facilely.

Z. Huang · Y. Chen (✉) · W. Zhou · Z. Guo
Institute of Polymers, Nanchang University, Xuefu Road 999, 330031 Nanchang, China
e-mail: ywchen@ncu.edu.cn

W. Zhou
e-mail: dramzwh@126.com

Therefore, they have wide range of potential applications as catalysts supports [1–3], drug/gene delivery carriers [4], medicine [5, 6], sensor [7, 8], separations [9] and imaging [10]. Especially, recent cytotoxicity studies on carbon nanotubes (CNTs) have shown that biocompatibility of nanomaterial might be mainly determined by surface functionalization rather than by size, shape, and material [11]. Thus, it is that inorganic nanotubes will be promising in the field of nanomedicine.

Various hollow nanotubes of carbon [12, 13], polymer [14], metals [15], and inorganic materials [16, 17] have been synthesized. Various facile or clever procedures have been developed to prepare these nanotubes, including rolling up layered materials [18], templating [19–22], sol–gel [23], chemical vapour deposition [24, 25], self-assembly [26, 27], atomic layer deposition [19], thermal evaporation–condensation–deposition [28]. But the general method is templating, based on coating shell onto templates, then by eliminating the core of core–shell nanostructure materials. In this method, polymer nanofibers [29], inorganic nanorods [30, 31], aluminum oxide [32], and aggregates of polymers or surfactants [26] have been used as core templates on which desired micro- or nanotubes have been formed. Finally, the hollow micro- and nanotubes were obtained via calcination or solvent extraction.

Electrospinning is a novel and efficient fabrication process that can be utilized to form polymer nanofibers. In the last years the interest for the production of polymer fibers ranging from 100 nm to 1 μm has grown. They are the efficient templates for preparation of nanotubes [29, 33].

A variety of hollow silica nanotubes have been synthesized by templating. Wang et al. [34] reported a facile synthesis of silica nanotubes, which were prepared by coating bismuth sulfide (Bi_2S_3) nanorods with silica, and immersing the products in HCl or focusing the electron beam on the heat-treated sample to remove templates. Yoon et al. [35] reported preparation of silica nanotubes via coating silica over the CdS nanorod templates and followed by selective photoetching of the core CdS nanorod templates. A series of silica nanotubes were prepared by immobilizing penicillin G acylase enzyme, glucose oxidase and lysozyme from needle-like calcium carbonate as templates [36–40]. By continuous oxidation of silicon nanowire arrays to give SiO_2 sheaths and removing core templates, SiO_2 nanotubes were created [21, 22]. The silica nano test tubes were synthesized by using alumina membranes as templates for application in bio-molecule delivery [41].

In this paper, we report the preparation of silica microfibers with poly(methyl methacrylate-*co*-vinylbenzyl chloride) [P(MMA-*co*-VBC)] microfibers as templates by step-by-step procedures as depicted in Scheme 1. P(MMA-*co*-VBC) was prepared by solution copolymerization of methyl methacrylate (MMA) and vinylbenzyl chloride (VBC) using 2,2′-azobis(isobutyronitrile) (AIBN) as the initiator. P(MMA-*co*-VBC) microfibers were prepared via electrospinning technique. In the second step, silyl groups were functionalized onto the P(MMA-*co*-VBC) microfiber surface by surface-initiated atom transfer radical polymerization (ATRP) of 3-(trimethoxysilyl)propyl methacrylate (TMSPM). A silica shell was then formed on the hybrid microfiber surface by hydrolysis and condensation of silyl functional groups with tetraethoxysilane (TEOS) in an ethanolic ammonia suspension. Hollow silica microtubes were finally obtained by thermal decomposition of the P(MMA-*co*-VBC) microtubes cores.

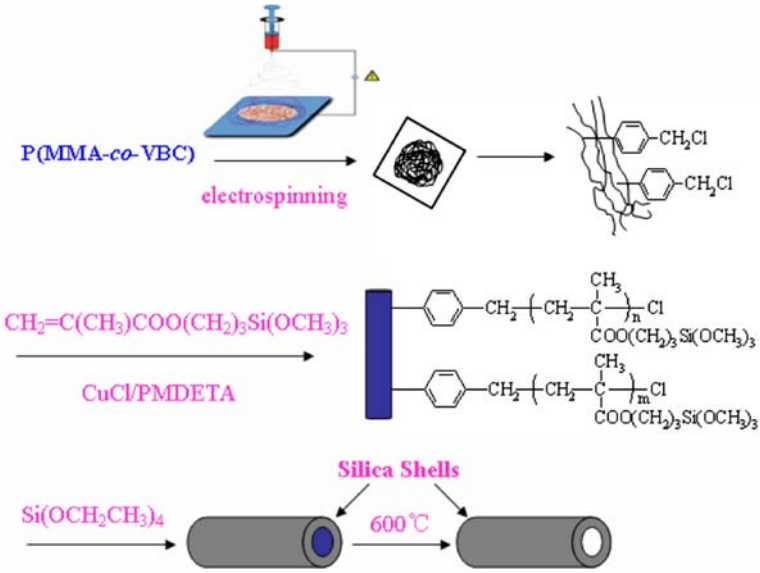

Scheme 1 Schematic illustration of the steps involved in the coating reaction of silyl-functionalized P(MMA-*co*-VBC) microfibers with silica and the formation of hollow silica microtubes

Experimental

Preparation of the P(MMA-co-VBC)

Solution polymerization of MMA and VBC (Aldrich, inhibitor removed) was carried out at 70 °C, using 2,2′-azobis(isobutyronitrile) (AIBN) as the initiator and toluene as the solvent. The monomer MMA (5 ml, 47.2 mmol) and VBC (2 ml, 14.2 mmol) were added into the 100 ml flask containing fresh distilled toluene (20 ml), and the solution was purged by argon for 15 min. After AIBN (0.03 g, 0.2 mmol) was added, the reaction mixture was heated under argon at 70 °C in an oil bath for 24 h. The solution was transferred into a 500 ml beaker. Methanol was added into the solution drop-wise, with vigorous stirring. The precipitated polymer was purified by re-precipitation with methanol from its chloroform solution. The purified polymer was then dried under reduced pressure at 70 °C. The number average molecular weight (M_n) and polydispersity were 38,000 and 1.34, respectively, determined by the gel permeation chromatography (GPC) with chloroform as eluent.

Preparation of the P(MMA-co-VBC) microfibers

The solution of P(MMA-co-VBC) in tetrahydrofuran (THF), 28% by weight, was prepared. Dodecylethyldimethylammonium bromide (DEDAB) (0.2 wt%) was added to improve the electrical conductivity. Then, the mixture was placed in a plastic syringe with a copper needle of 14 cm in length and 0.7 mm in diameter. An electrode was clamped on the needle and connected to a power supply, which could

generate a direct-current (d_c) voltage up to 30 kV. In this experiment, a voltage of 15 kV was applied. A flat aluminum collector was placed 15 cm below the tip of the needle to collect the fibers. Electrospinning was performed at room temperature in air, and the feeding rate of the solution was 1.2 ml h^{-1}.

Silyl-functionalization of the P(MMA-co-VCB)-microfibers

In this step, surface-initiated atom transfer radical polymerization (ATRP) on the VBC copolymer (P(MMA-*co*-VCB)) microfibers was performed. A 100 ml flask was charged with the P(MMA-*co*-VCB) microfibers (25 mg) and ethanol (10 ml). Dry argon was bubbled through the mixture for 15 min to remove oxygen from the polymerization system. After removal of oxygen, CuCl (8 mg, 0.08 mmol; Aldrich, 99%), *N*,*N*,*N*′,*N*′,*N*″-pentamethyldiethylenetriamine (70 μl, 0.48 mmol; PMDETA, Aldrich, 99%), and 3-(trimethoxysilyl) propyl methacrylate (1 ml, 4.2 mmol; TMSPM, Aldrich, 98%) were added to the same reaction mixture. Argon was bubbled through the mixture for another 20 min to ensure the complete removal of oxygen. The flask was then sealed with a high-temperature silicon rubber septum. The mixture was sonicated for 2 min to accelerate the dissolution of the reactants into ethanol and the dispersion of the microfibers in the reaction mixture. The reaction was allowed to proceed at room temperature under stirring. The polymerization time was varied from 6 to 24 h to produce polymer shells of different thickness. The TMSPM polymer-coated P(MMA-*co*-VCB) microfibers were recovered from the suspension by centrifugation. They were washed several times by centrifuging/redispersion cycles in ethanol.

The silica-coated P(MMA-co-VCB) microfibers

In a typical experiment to form the outer silica layer, surface-functionalized P(MMA-*co*-VCB) microfibers (0.3 g) were suspended in an ethanol/water mixture (80:20; 100 ml) containing ammonium hydroxide (0.4 mol l^{-1}). Tetraethoxysilane (1.6 g, 10.5 mmol; TEOS, Aldrich) was dissolved in ethanol (5 ml). The TEOS solution was then added dropwise to the ethanolic ammonia suspension under magnetic stirring at room temperature. The silica-coated microfibers were dispersed in copious amounts of ethanol, recovered by centrifugation, and finally dried at 70 °C.

Formation of the hollow silica microfibers

The microfibers so obtained were heated at 600 °C in the muffle furnace for 4 h to decompose the P(MMA-*co*-VCB) cores and to produce the hollow silica microfibers. The calcined product was stored as a colloidal dispersion in ethanol.

Characterization

FTIR spectra of the specimens dispersed in KBr disks were recorded on a SHIMADZU IRprestige-21 spectrophotometer. Scanning electron microscope

(SEM) was performed using a JEOL HITACHI S-3000N SEM at an accelerating voltage of 5 kV. Samples were mounted on an aluminum alloy stub and sputter-coated with gold to improve conductivity. Transmission electron microscope (TEM) analysis was used to characterize the microfibers morphology. In a typical experiment, several drops of the colloidal dispersion were introduced on to a carbon film supported by a copper grid. The droplet was allowed to dry in air, and then observed under a JEM-2010HR TEM operating at an acceleration voltage of 100 kV. X-ray diffraction (XRD) pattern was recorded on a Bruker D8 Focus X-ray diffractometer, equipped with Ni-filtered Cu K_α radiation in the reflection mode with a wavelength of 0.154 nm. The scanning 2θ angle ranged between 5° and 75° with a step scanning rate of 2° min^{-1}. Thermal Gravimetric Analysis (TGA) was performed under nitrogen with a Perkin-Elmer TGA7 at a heating rate 20 °C min^{-1}. The X-ray photoelectron spectroscopy (XPS) was performed on a Kratos AXIS HSi spectrometer with a monochromatized Al K_α X-ray source (1486.71 eV photons) at a constant dwelling time of 100 ms and a pass energy of 40 eV. The anode current was 15 mA. The pressure in the analysis chamber was maintained at 5×10^{-8} Torr or lower during the measurement.

Results and discussion

The absorption bands specific to P(MMA-*co*-VBC) microfibers at 751, 1,450, 1,511, 1,607 and 1,732 cm^{-1} can be readily identified in the FTIR spectrum of Fig. 1a. The presence of P(MMA-*co*-VBC) microfibers, about 1 μm in diameter, is revealed by the SEM image shown in Fig. 2a. Energy-dispersive X-ray (EDX) analysis of a

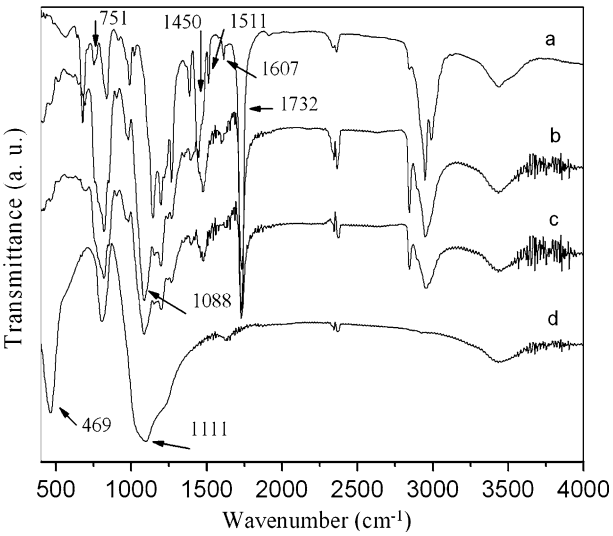

Fig. 1 FT-IR spectra of **a** the P(MMA-*co*-VBC) microfibers, **b** the silyl-functionalized microfibres after ATRP for 24 h, **c** the silica-coated microfibers, **d** the hollow silica microtubes

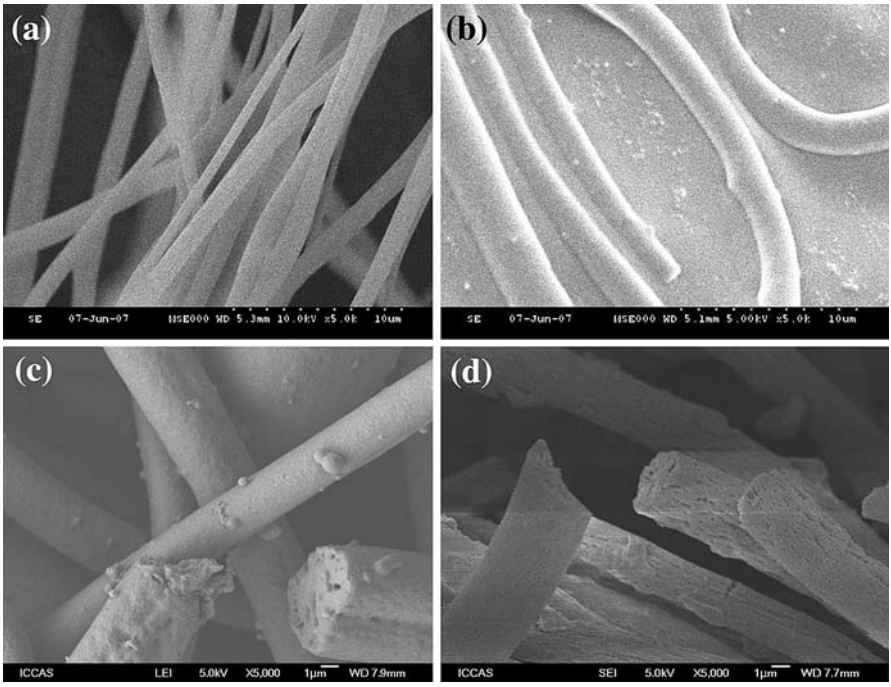

Fig. 2 SEM images of **a** the P(MMA-*co*-VBC) microfibers, **b** the silyl-functionalized microfibers after ATRP for 24 h, **c** the silica-coated microfibers, and **d** the hollow silica microtubes

number of nanofibers shown in Fig. 3a was carried out to elucidate the chemical composition of the surface. The EDX signals at 0.25 keV (attributable to carbon) and at 2.65 keV (attributable to chlorine) are consistent with the presence of P(MMA-*co*-VBC). The signals at 1.28, 1.55 and 2.20 keV arise from the aluminum alloy stub and the sputter-coated gold used for the SEM obserbvation. The TGA thermogram of the P(MMA-*co*-VBC) microtubes showed complete decomposition as heating to 600 °C (Fig. 5a). The XPS analysis was performed to characterize the near-surface compositions of the microfibers. As is shown in Fig. 7a, the peaks at 532 and 285 eV are attributable to O 1*s* and C 1*s*, respectively. The peaks at 270 and 200 eV should be ascribed to Cl 2*s* and Cl 2*p*, respectively. The component of the microfibers is associated with the presence of P(MMA-*co*-VBC). However, peaks at 153 and 102 eV, ascribed to Si 2*s* and 2*p*, respectively, are also observed in the spectrum. It should be due to the contamination of the P(MMA-*co*-VBC) microfibers, arising from the XPS measurements.

Benzyl chloride ($-C_6H_4-CH_2Cl$) has been used previously for grafting polymers to solid surfaces, or for preparing polymers in solution [42, 43]. Although the benzyl chloride of P(MMA-*co*-VBC) is not an efficient initiating group for ATRP, its performance is acceptable in the present surface-initiated ATRP of TMSPM. Polymer growth was confined, as expected, to the surface of P(MMA-*co*-VBC) microfibers. The FTIR spectra of the silyl-functionalized microfibers showed absorption bands corresponding to both P(MMA-*co*-VBC) and grafted TMSPM

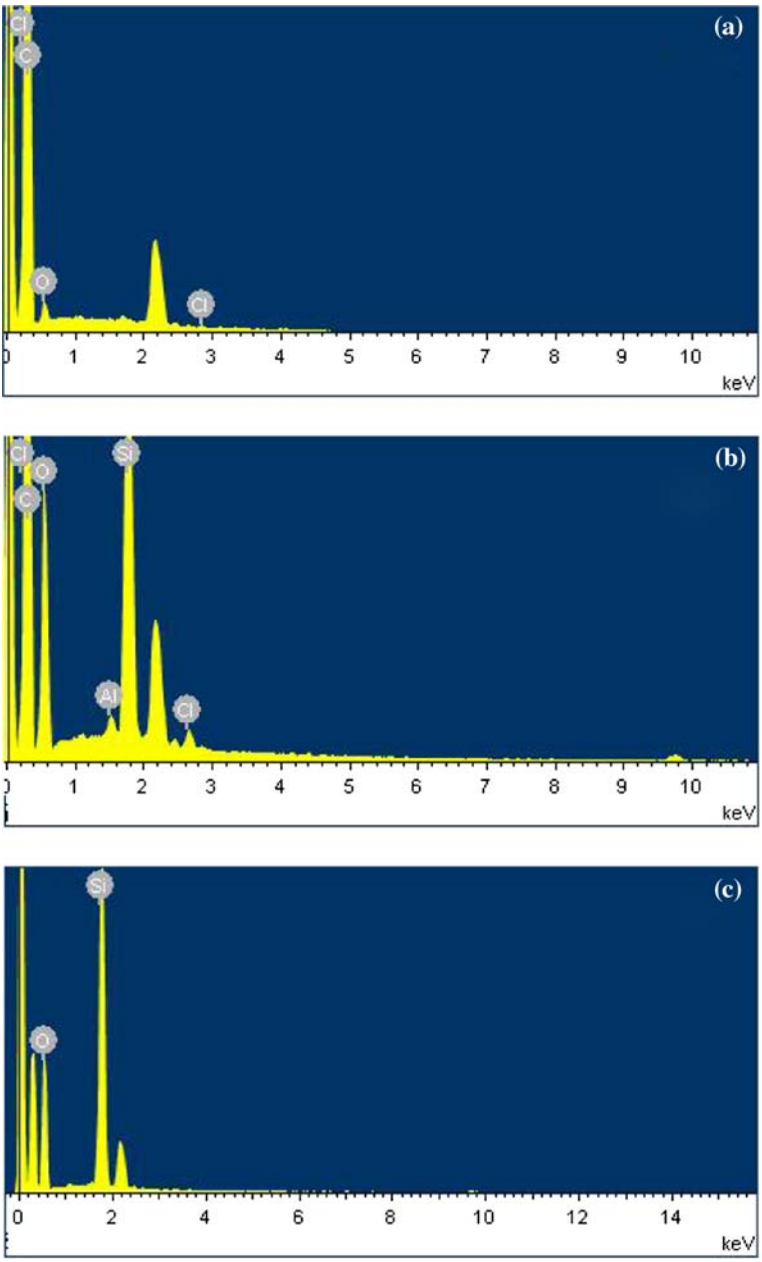

Fig. 3 EDX spectra of **a** the P(MMA-*co*-VBC) microfibers, **b** the silyl-functionalized microfibers after ATRP 6 h, **c** the hollow silica microtubes

polymer. Spectra revealed the presence of absorption bands corresponding to the grafted TMSPM polymer at 1,088 cm^{-1}, in addition to the absorption bands specific to P(MMA-*co*-VBC) at 1,607, 1,511 and 751 cm^{-1}, for the silyl-functionalized

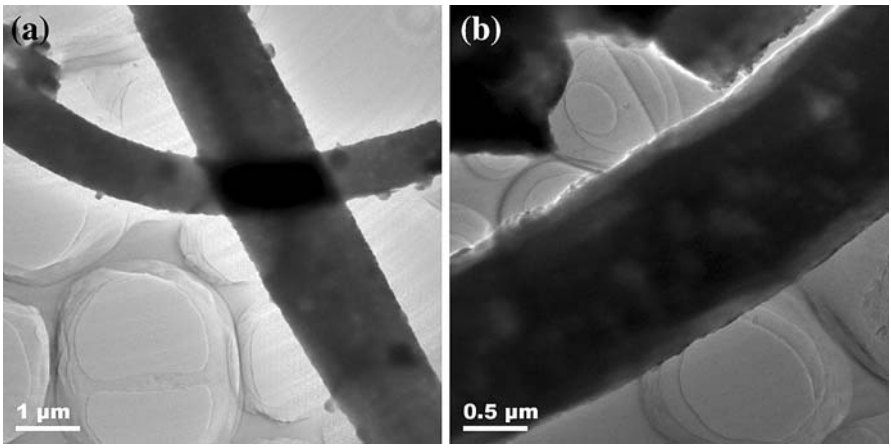

Fig. 4 TEM images of **a** the P(MMA-*co*-VBC) microfibers and **b** the hollow silica microtubes

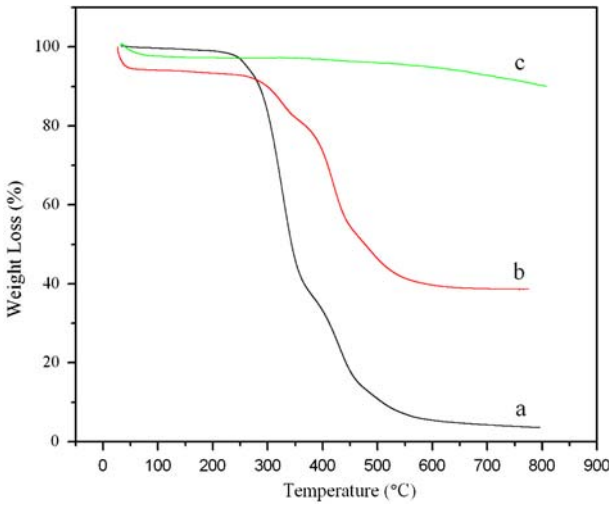

Fig. 5 TGA thermograms of the **a** the P(MMA-*co*-VBC) microfibers, **b** the silica-coated microfibers, **c** the hollow silica microtubes

microfibers as shown in Fig. 1b. The absence of the C=C vibration band at 1,634 cm^{-1} confirms polymerization of the TMSPM monomer, and that the polymer chains are chemically anchored onto the P(MMA-*co*-VBC) surface. After surface functionalization by ATRP for 24 h, no obvious change in shape of the microfibers was observed, but the diameter of the microfibers increased, as shown in SEM image (Fig. 2b). EDX signal at 1.74 keV is consistent with the appearance of silicon in silyl-functionalized polymer (Fig. 3b). The carbon and chlorine signals are also discernible. The near-surface compositions of the silyl-functionalized microfibers is different from that of the P(MMA-*co*-VBC) microfibers, as observed

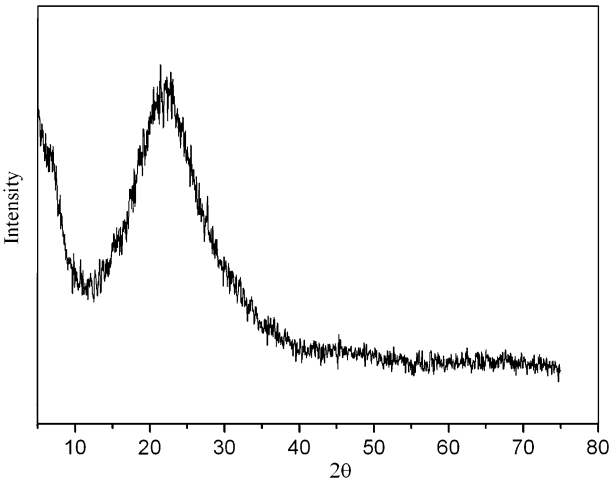

Fig. 6 X-ray spectra of the hollow microtubes

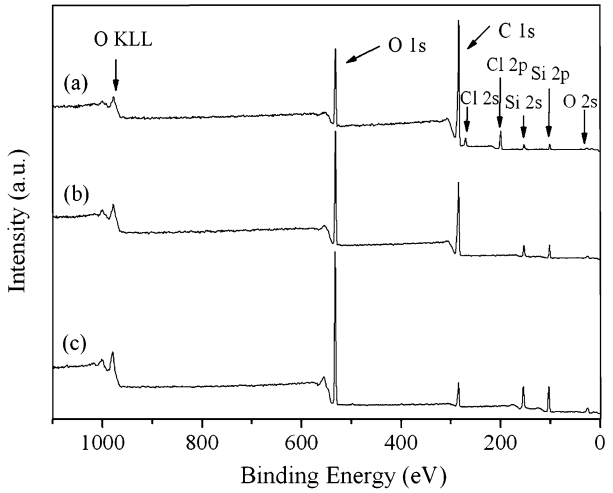

Fig. 7 XPS spectrums of **a** the P(MMA-*co*-VBC) microfibers, **b** the silyl-functionalized microfibres after ATRP for 24 h, **c** the hollow silica microtubes

from Fig. 7b. The XPS spectrum consists of peaks at 532, 285, 153 and 102 eV, attributable to O 1*s*, C 1*s*, Si 2*s* and Si 2*p*, respectively. The peaks ascribed to Cl 2*s* and Cl 2*p* disappeared, indicating that the P(MMA-*co*-VBC) microfibers were covered by the TMSPM polymer of a thickness of more than 10 nm. The efficiency of the surface-initiated ATRP represents the amount of the TMSPM grafted onto the P(MMA-*co*-VCB) microfibers. It can be calculated based on the intensity ratio between silicon signal and chlorine signal as revealed in XPS analysis. As the ATRP time increasing, the molecular weight of the grafted copolymer increased, resulting in the thickness growth of the grafted polymer consequently increased thickness of

silica shell after sol–gel process. In XPS analysis, the intensity of chloride decreased with comparison to increase of the intensity of the silicon. However, the quantitative calculation is not performed in this article as the chloride intensity is too weak to determine in the XPS analysis after ATRP for 24 h due to limitation of XPS detection depth.

The trimethoxysilyl groups on the silyl-functionalized microfibers were treated with TEOS in ethanol containing 20 wt% water under basic condition to yield the silica-coated microfibers. As shown in the FTIR spectrum of Fig. 1c, characteristic bands of Si–O–Si bonds at about 469 and 1,111 cm^{-1} might be obscured by the large existence of silyl-functionalized P(MMA-co-VBC) polymer. SEM image of Fig. 2c shows a coarse surface of the silica-coated microfibers. Figure 5b exhibits the TGA thermogram of the silica-coated microfibers. After heating to 750 °C, there still existed 39% residue, by weight, attributable to the SiO_2. Three weight loss stages are observed on the TGA curve. The stage below 100 °C corresponds to the evaporation of small molecules such as water and ethanol. In addition, the stage between 270 and 340 °C corresponds to the decomposition of the PMMA segments, while the stage above 340 °C corresponds to the decomposition of PVBC segments. The remaining residue should be assigned to SiO_2, confirming that silica has been introduced on to the microfibers.

Due to the hydrophobic character of P(MMA-*co*-VBC) microfibers, TEOS can readily diffuse into the composite-polymer microfibers and chemically react with the methoxy or hydroxyl groups. The alcohols produced by the hydrolysis and condensation reactions may, in turn, help to increase the solubility of TEOS in the microfibers. Polycondensation is thus promoted by a high local concentration of TEOS and by the silyl groups on the hybrid core.

In the final step, the P(MMA-*co*-VBC) core was removed from the microfibers, by calcinations at 600 °C in air, to give rise to the hollow silica microtubes. The microtubes were dispersed in water by ultrasonification. The diameter of the hollow silica microtubes was very close to that of the silica-coated microfibers. The SEM image of Fig. 2d shows the porous microfibers, indicating that decomposition and oxidation have taken place during the calcinations process. The TEM image of Fig. 4b clearly reveals the hollow structure of the silica microtubes with a silica shell of about 0.25 μm in thickness, as compared with the solid microfibers shown in Fig. 4a. Additionally, FTIR and chemical analysis results confirmed that the P(MMA-*co*-VBC) core has been quantitatively removed from the composite microfibers. The FTIR spectrum of the hollow silica microtubes (Fig. 1d) is similar to that of pure silica. The EDX spetrum of the hollow silica microtubes (Fig. 3c) confirmed the presence of only silicon and oxygen, with a Si/O ratio of approximately 1:2. Figure 5c shows the TGA thermogram of the hollow silica microtubes. Less than 5% weight loss is observed as heating to 800 °C, suggesting that the microtubes were mainly composed of SiO_2. Only one diffraction reflection at $2\theta = 22.7°$ was observed in the XRD spectra (Fig. 6), indicating that the silica in the microtubes was amorphous. The XPS results shown in Fig. 7c indicate that the microtubes are mainly composed of Si and O, although the minor peak at 285 eV, ascribed to C 1*s*, could still be discerned. The peak of C 1*s* should arise from the contamination during the measurement. Additionally, the peaks of Si 2*s* and Si 2*p*

present a higher area in comparison to the P(MMA-*co*-VBC) microfibers and silyl-functionalized microfibers, showing an increase of silicon in composition. It is believed that silica was anchored on the microfibers.

Conclusions

The silica microtubes were successfully prepared by a step-by-step procedure, via (1) preparation of the P(MMA-*co*-VBC) microfibers, (2) surface-initiated ATRP of TMSPM on the microfiber templates, (3) polycondensation with TEOS to form a silica shell, and (4) removal of the P(MMA-*co*-VBC) core by thermal decomposition. The thickness of silica microtubes is about 0.25 μm, and the silica microtubes are confirmed to be amorphous. It is possible to produce microtubes containing a variety of inorganic layers by using different sol–gel precursors and different monomers for ATRP.

Acknowledgments Financial support for this work was provided by the National Natural Science Foundation of China (50773029), the Fok Ying Tong Education Foundation (101047), the program for New Century Excellent Talents in University (NCET-06-0574), Jiangxi Provincial Department of Education, and the Program for Innovative Research Team of Nanchang University.

References

1. Xu YH, Lin XQ (2007) Selectively attaching Pt-nano-clusters to the open ends and defect sites on carbon nanotubes for electrochemical catalysis. Electrochim Acta 52:5140
2. Izabela J, Gauthier W, Ledoux MJ, Cuong PH (2007) Structured silica reactor with aligned carbon nanotubes as catalyst support for liquid-phase reaction. J Mol Catal A: Chem 267:92
3. Lee SY, Yamada M, Miyake M (2005) Synthesis of carbon nanotubes over gold nanoparticle supported catalysts. Carbon 43:2654
4. Bianco A, Kostarelos K, Partidos CD, Prato M (2005) Biomedical application of functionalised carbon nanotubes. Chem Commun 5:571
5. Wang JX, Wen LX, Wang ZH, Chen JF (2006) Immobilization of silver on hollow silica nanospheres and nanotubes and their antibacterial effects. Mater Chem Phys 96:90
6. Son SJ, Bai X, Nan AJ, Ghandehari H, Lee SB (2006) Template synthesis of multifunctional nanotubes for controlled release. J Control Release 114:143
7. Wang D, Chen LW (2007) Temperature and pH-responsive single-walled carbon nanotube dispersions. Nano Lett 7:1480
8. He B, Son SJ, Lee SB (2006) Shape-coded silica nanotubes for biosensing. Langmuir 22:8263
9. Yang HH, Zhang SQ, Yang W, Chen XL, Zhuang ZX, Xu JG, Wang XR (2004) Molecularly imprinted sol-gel nanotubes membrane for biochemical separations. J Am Chem Soc 126:4054
10. Xu ZX, Hu PA, Wang SM, Wang XB (2008) Biological functionalization and fluorescent imaging of carbon nanotubes. Appl Surf Sci 254:1915
11. Sayes CM, Liang F, Hudson JL, Mendez J, Guo WH, Beach JM, Moore VC, Doyle CD, West JL, Billups WE, Ausman KD, Colvin VL (2006) Functionalization density dependence of single-walled carbon nanotubes cytotoxicity in vitro. Toxicol Lett 161:135
12. Fu QG, Wang ZW, Li KZ (2007) In situ catalytic growth of carbon nanotubes on the surface of carbon cloth. Compos Sci Technol 67:2986
13. Inoue T, Gunjishima I, Okamoto A (2007) Synthesis of diameter-controlled carbon nanotubes using centrifugally classified nanoparticle catalysts. Carbon 45:2164
14. Zhang ZM, Wei ZX, Zhang LJ, Wan MX (2005) Polyaniline nanotubes and their dendrites doped with different naphthalene sulfonic acids. Acta Mater 53:1373

15. Ma H, Tao ZL, Gao F, Chen J (2004) Template synthesis of transition-metal Ru and Pd nanotubes. Chin J Inorg Chem 10:1187
16. Duan JX, Huang XT, Wang EK (2006) PEG-assisted synthesis of ZnO nanotubes. Mater Lett 60:1918
17. Li T, Sun CG, Fan ML, Huang CJ, Wu HL, Chao ZB, He ZS (2006) A redox-assisted supramolecular assembly of manganese oxide nanotube. Mater Res Bull 41:2035
18. Schmidt OG, Eberl K (2001) Nanotechnology: thin solid films roll up into nanotubes. Nature 410:168
19. Ras RHA, Kemell M, Wit JD, R M, Brinke GT, Leskelä M, Ikkala O (2007) Hollow inorganic nanospheres and nanotubes with tunablewall thicknesses by atomic layer deposition on self-assembled polymeric templates. Adv Mater 19:102
20. Nakane K, Shimada N, Ogihara T, Ogata N, Yamaguchi (2007) Formation of TiO_2 nanotubes by thermal decomposition of poly(vinyl alcohol)-titanium alkoxide hybrid nanofibers. J Mater Sci 42:4031
21. Mulvihill MJ, Rupert BL, He RR, Hochbaum A, Arnold J, Yang PD (2005) Synthesis of bifunctional polymer nanotubes from silicon nanowire templates via atom transfer radical polymerization. J Am Chem Soc 127:16040
22. Fan R, Wu YY, Li DY, Yue M, Majumdar A, Yang PD (2003) Fabrication of silica nanotube arrays from vertical silicon nanowire templates. J Am Chem Soc 125:5254
23. Nakamura H, Matsui Y (1995) Silica gel nanotubes obtained by the sol–gel method. J Am Chem Soc 117:2651
24. Griffiths H, Xu C, Barrass T, Cookem M, Vereecken P, Esconjauregui S (2007) Plasma assisted growth of nanotubes and nanowires. Surf Coat Technol 201:9215
25. Porro S, Musso S, Giorcelli M, Chiodoni A, Tagliaferro A (2007) Optimization of a thermal-CVD system for carbon nanotube growth. Physica E 37:16
26. Tai GA, Guo WL (2007) Sonochemical preparation of nickel alumina nanotubes templated by anionic surfactant assemblies. J Mater Sci 42:10245
27. Wang JX, Wen LX, Liu RJ, Chen JF (2005) Needle-like calcium carbonate assisted self-assembly of mesostructured hollow silica nanotubes. J Solid State Chem 178:2383
28. Stasio SD (2004) Growth of zinc hollow nanofibers and nanotubes by thermal evaporation-condensation-deposition route. Chem Phys Lett 393:498
29. Ras RHA, Ruotsalainen T, Laurikainen K, Linder MB, Ikkala O (2007) Hollow nanoparticle nanotubes with a nanoscale brick wall structrue of clay mineral platelets. Chem Commun 13:1366
30. Obare SO, Jana NR, Murphy CJ (2001) Preparation of polystyrene- and silica-coated gold nanorods and their use as templates for the synthesis of hollow nanotubes. Nano Lett 1:601
31. Limmer SJ, Chou TP, Cao GZ (2003) Formation and optical properties of cylindrical gold nanoshells on silica and titania nanorods. J Phys Chem B 107:13313
32. Zhang GY, Guo B, Chen J (2006) Mco_2O_4(M=Ni,Cu,Zn) nanotubes: template synthesis and application in gas sensors. Sens Actuators B: Chem 114:402
33. Pan C, Ge LQ, Gu ZZ (2007) Fabrication of multi-walled carbon nanotube reinforced polyelectrolyte hollow nanofibers by electrospinning. Compos Sci Technol 67:3271
34. Wang SF, Gu F, Yang ZS, Lü MK, Zhou GJ, Zou WG (2005) Facile synthesis of silica-coated Bi_2S_3 nanorods and hollow silica nanotubes. J Cryst Growth 282:79
35. Yoon JH, Chae WS, Cho HM Choi MG, Kim YR (2006) Novel fabrication of silica nanotube by selective photoetching of CdS nanorod template. Mater Res Bull 41:1657
36. Xiao QG, Tao X, Chen JF (2007) Silica nanotubes based on needle-like calcium carbonate: fabrication and immobilization for glucose oxidase. Ind Eng Chem Res 46:459
37. Wang JX, Wen LX, Wang ZH, Wang M, Shao L, Chen JF (2004) Facile synthesis of hollow silica nanotubes and their application as supports for immobilization of silver nanoparticles. Scr Mater 51:1035
38. Ding HM, Shao L, Liu RJ, Xiao QG, Chen JF (2005) Silica nanotubes for lysozyme immobilization. J Colloid Interface Sci 290:102
39. Xiao QG, Tao X, Zhang JP, Chen JF (2006) Hollow silica nanotubes for immobilization of penicillin G acylase enzyme. J Mol Catal B: Enzym 42:14
40. Xiao QG, Tao X, Zou HK, Chen JF (2008) Comparative study of solid silica nanoparticles and hollow silica nanoparticles for the immobilization of lysozyme. Chem Eng J 137:38
41. Gasparac R, Kohi P, Mota MO, Trofin L, Martin CR (2004) Template synthesis of nano test tubes. Nano Lett 4:513

42. Wang JS, Matyjaszewski K (1995) Controlled/living radical polymerization. Halogen atom transfer radical polymerization promoted by a Cu(I)/Cu(II) redox process. Macromolecules 28:7901
43. Huang X, Doneski LJ, Wirth M (1998) Surface-confined living radical polymerization for coatings in capillary electrophoresis. J Anal Chem 70:4023